Taylor & Francis
Taylor & Francis Group

BRIEF REPORT

☾ OPEN ACCESS | Check for updates

Neoadjuvant chemoradiation alters the immune microenvironment in pancreatic ductal adenocarcinoma

Robyn D. Gartrell[a]*, Thomas Enzler[b]*, Pan S. Kim[c], Benjamin T. Fullerton[d], Ladan Fazlollahi[e], Andrew X. Chen[f], Hanna E. Minns[a], Subha Perni[g], Stuart P. Weisberg[e], Emanuelle M. Rizk[d], Samuel Wang[d], Eun Jeong Oh[h], Xinzheng V. Guo[d], Codruta Chiuzan [iD][i], Gulam A. Manji[d], Susan E. Bates[d], John Chabot[j], Beth Schrope[j], Michael Kluger[j], Jean Emond[j], Raul Rabadán[k], Donna Farber[l], Helen E. Remotti[e], David P. Horowitz[m], and Yvonne M. Saenger[n]

[a]Department of Pediatrics, Columbia University Irving Medical Center, New York, NY, USA; [b]Rogel Cancer Center, University of Michigan Medicine, Ann Arbor, MI, USA; [c]Department of Medicine, University of Pittsburgh Medical Center, Pittsburgh, PA, USA; [d]Department of Medicine, Columbia University Irving Medical Center, New York, NY, USA; [e]Department of Pathology, Columbia University Irving Medical Center, New York, NY, USA; [f]Vagelos College of Physicians and Surgeons, Columbia University, New York, NY, USA; [g]Harvard Radiation Oncology Program, Massachusetts General Hospital and Brigham and Women's Hospital/Dana-Farber Cancer Institute, Boston, MA, USA; [h]Mailman School of Public Health, Columbia University, New York, NY, USA; [i]Department of Biostatistics, Columbia University Irving Medical Center, New York, NY, USA; [j]Department of Surgery, Columbia University Irving Medical Center, New York, NY, USA; [k]Department of Systems Biology, Columbia University Irving Medical Center, New York, NY, USA; [l]Department of Microbiology and Immunology, Columbia University Medical Center, New York, NY, USA; [m]Department of Radiation Oncology, Columbia University Irving Medical Center, New York, NY, USA; [n]Albert Einstein College of Medicine, Columbia University

ABSTRACT

Patients with pancreatic ductal adenocarcinoma (PDAC) have a grim prognosis despite complete surgical resection and intense systemic therapies. While immunotherapies have been beneficial with many different types of solid tumors, they have almost uniformly failed in the treatment of PDAC. Understanding how therapies affect the tumor immune microenvironment (TIME) can provide insights for the development of strategies to treat PDAC. We used quantitative multiplexed immunofluorescence (qmIF) quantitative spatial analysis (qSA), and immunogenomic (IG) analysis to analyze formalin-fixed paraffin embedded (FFPE) primary tumor specimens from 44 patients with PDAC including 18 treated with neoadjuvant chemoradiation (CRT) and 26 patients receiving no treatment (NT) and compared them with tissues from 40 treatment-naïve melanoma patients. We find that relative to NT tumors, CD3$^+$ T cell infiltration was increased in CRT treated tumors (p = .0006), including increases in CD3$^+$CD8$^+$ cytotoxic T cells (CTLs, p = .0079), CD3$^+$CD4$^+$FOXP3$^-$ T helper cells (T$_h$, p = .0010), and CD3$^+$CD4$^+$FOXP3$^+$ regulatory T cells (Tregs, p = .0089) with no difference in CD68$^+$ macrophages. IG analysis from micro-dissected tissues indicated overexpression of genes involved in antigen presentation, T cell activation, and inflammation in CRT treated tumors. Among treated patients, a higher ratio of Tregs to total T cells was associated with shorter survival time (p = .0121). Despite comparable levels of infiltrating T cells in CRT PDACs to melanoma, PDACs displayed distinct spatial profiles with less T cell clustering as defined by nearest neighbor analysis (p < .001). These findings demonstrate that, while CRT can achieve high T cell densities in PDAC compared to melanoma, phenotype and spatial organization of T cells may limit benefit of T cell infiltration in this immunotherapy-resistant tumor.

Introduction

Pancreatic ductal adenocarcinoma (PDAC) is a devastating disease with a 5-year survival of only 10.8%.[1] With estimated 48,220 people dying from PDAC in the U.S. in 2021 it is currently the third most common cause of cancer-related death.[1] PDAC is predicted to become the second leading cause of cancer-related death, surpassing colorectal cancer by 2030.[2] Only 20% of patients with PDAC have disease that can be surgically resected at diagnosis, with surgical feasibility generally defined based on the extent of tumor contact with key vascular structures and the absence of distant metastasis.[3] Unfortunately, even if complete resection is successfully achieved and maximum adjuvant chemotherapy treatment is subsequently given, the majority of patients will ultimately relapse and die.[4,5] Of numerous available systemic therapies, only FOLFIRINOX [fluorouracil, leucovorin, irinotecan, oxaliplatin] and gemcitabine with capecitabine have demonstrated a significant improvement in overall survival (OS) in the adjuvant setting.[5,6] More recently, preoperative delivery of therapy in PDAC has gained momentum because borderline resectable and/or even locally advanced tumors can eventually be downstaged into resectable tumors.[3,7,8] Preoperative treatment also significantly decreases the likelihood of having microscopic or macroscopic residual tumors after resection, and it may help to eradicate systemic occult disease.

PDAC is highly aggressive and therefore intensive systemic cytotoxic therapies, radiation, and/or chemoradiation therapies are routinely given to virtually all patients receiving neoadjuvant treatment. Reliance on conventional therapies exists because options such as immunotherapy have been largely unsuccessful.[9,10] By contrast, other tumors such as melanoma exhibit beneficial and often durable responses to immunotherapy in the adjuvant and metastatic settings.[11–14] In contrast to melanoma, PDACs have the ability to generate and maintain a particularly immunosuppressive tumor immune microenvironment (TIME), which may explain the lack of efficacy of immunotherapies.[9,15] Structurally, the TIME of PDAC is characterized by a unique and very dense fibrotic desmoplastic stromal reaction generated by activated fibroblasts and myofibroblasts.[16] This dense stroma forms a mechanical barrier that may limit the penetration of drugs and effector immune cells to the tumor site.[17] By contrast, tumor-associated macrophages (TAMs) and myeloid-derived suppressor cells (MDSCs) in PDAC have been shown to better penetrate the tissue and directly promote tumor growth by contributing to an immunosuppressive microenvironment. These cell populations establish this environment by secreting amino acid-degrading enzymes, which result in anergy of cytotoxic T cells (CTLs) and T helper cells (T_h) and the accumulation of T regulatory cells (T_{regs}).[18–23] Interestingly, there is evidence to suggest that certain immune characteristics of PDAC correlate with survival leading one to speculate whether immunomodulation of the TIME has a role.[24] In this regard, phenotypes of PDAC have correlated with prognosis, including an "immune escape" type, defined by high infiltration of FOXP3+ T_{regs} and decreased numbers of other lymphocyte subsets.[25] This is consistent with other reports showing that T_{reg} infiltration in the TIME of PDAC patients is associated with poor prognosis.[26–29]

Understanding the effect of immunosuppression in PDAC and how it is altered by current therapies is critical design efficient combination therapeutic approaches to improve survival.[30] While studies in mouse models have demonstrated a favorable impact of radiation on the TIME in PDAC, the impact of neoadjuvant CRT on human PDAC and on the associated TIME is not well established.[31] In our study, we evaluate the impact of neoadjuvant CRT on the TIME in PDAC by quantitative multiplex immunofluorescence (qmIF) with quantitative spatial analysis (qSA) and immunogenomic (IG) analysis and compared to non-treat (NT) cases. We demonstrate that CRT leads to an influx of T cells, specifically CTLs, T_h cells and Tregs, into the TIME. Moreover, we show that CRT is associated with an upregulation of genes involved in inflammatory processes and antigen-presentation. Predominance of Tregs in CRT treated tumors correlates with poor outcome. Further, we find that the influx of CD3 + T cells and CD3+ CD8+ cytotoxic T cells into the TIME of CRT PDAC is not significantly different from infiltration levels found in treatment-naive melanoma, but, in contrast with melanoma, neither CD3+ nor CD3+ CD8+ cells correlate with a favorable prognosis in CRT PDAC. Spatial organization of the T cells is different between PDAC and melanoma with T cells in melanoma forming large clusters in tumor associated stroma whereas T cells in PDAC are dispersed diffusely within the tumor and peri-tumoral stroma.

Materials and methods

Patients and samples

The study was approved by Columbia University Irving Medical Center's (CUIMC) Institutional Review Board (IRB). We created a retrospective database of PDAC patients treated at CUIMC by searching surgical pathology records from 2011 to 2018 and screening for available tissues. Only patients with available baseline, treatment, and post-treatment clinical data were included. Patients were excluded for incomplete documentation, histology not consistent with PDAC, second primary, recurrent cancer, palliative intent, and treatment at outside hospital. One patient was excluded because resection occurred 11 months following CRT whereas all of the other patients received resection between 1 and 3 months following CRT. Neoadjuvant radiotherapy was delivered via either intensity-modulated radiotherapy (IMRT), with patients receiving 50.4 Gy in 28 fractions of 1.8 Gy/fraction with concurrent capecitabine, or stereotactic body radiotherapy (SBRT), with patients receiving 33 Gy in 5 fractions of 6.6 Gy/fraction (Supplemental Figure S1). We also compare specimens from PDAC to melanoma. Clinical data on these primary melanoma patients is included in the supplement (Supplemental Table 6).

For included patients, hematoxylin and eosin (H&E) slides were reviewed by board-certified gastrointestinal (GI) pathologists (LF and HR). Clinical criteria were met in 53 patients with 44 patients having confirmed tumors by H&E, excluding 9 patients with no tumor in the specimen. During the qmIF staining process, 13 were lost due to tissue destruction or staining artifact and were unable to be analyzed using the image analysis software, leaving a total of 31 analyzable samples for qmIF. Ten patients had enough specimen for qmIF but not enough specimen for RNA extraction. Of the 13 cases that could not be analyzed using qmIF, all could be RNA extracted leaving a total of 34 patients analyzed by IG, including 21 patients analyzed using both qmIF and IG. Normal pancreas tissue samples for control were collected from deceased organ donors as part of organ acquisition for clinical transplantation through an approved protocol and material transfer agreement with LiveOnNY, as described previously.[32,33] Samples from donors were free of cancer, chronic diseases, seronegative for hepatitis B, C, and HIV and were age and sex matched to tumor cases. Use of organ donor tissues are not classified as "human subjects" by CUIMC IRB as these samples were taken from brain-dead (deceased) individuals.

Quantitative multiplex immunofluorescence (qmIF)

Full-section 5-um slides of formalin-fixed paraffin embedded (FFPE) tissue specimens were stained using Opal™ multiplex 6-plex kits, according to the manufacturer's protocol (PerkinElmer/Akoya), for DAPI, CD3 (clone LN10; Leica; 1:150 dilution), CD4 (clone 4SM95; 1:1000) CD8 (clone 4B11; Leica; 1:2RTU), FOXP3 (clone 236A/E7; abcam; 1:300), CD68 (clone KP1; Biogenex, ready to use); Ki67 (clone MIB1; Dako; ready to use). Single stain controls and an unstained slide were also included to create a multispectral library as previously described.[34]

H&E slides were viewed by a GI pathologist to determine representative areas for multispectral images captured with 20X objective using Vectra (PerkinElmer/Akoya). Regions of interest (ROI) were approximately 700 × 520 um. Images were analyzed using inForm software version 2.4.1 (PerkinElmer/Akoya), as per protocol previously defined, by investigators blinded to treatment status.[34] Briefly, five representative areas for each slide were randomly selected in the tumor area as determined by a GI pathologist, and each image was factored equally into the analysis for each patient. Tissue segmentation was performed by highlighting examples of tumor and stroma based on morphology and Ki-67 expression under supervision of a board-certified GI pathologist (LF) to evaluate the composition of the tissue in terms of tumor and stromal components. Images were then processed for cell segmentation using the nuclear marker, DAPI, then phenotyped for tumor, CD3, CD68, and other, and then scored using a threshold for positivity for CD4, FOXP3, CD8, Ki67 as previously described.[34] Data exported from inForm (Akoya) then concatenated and analyzed using the phenoptr package (Akoya) in R (v 4.0.2).

RNA extraction and processing

FFPE blocks were obtained for 34 PDAC patients and 12 normal pancreas controls. For each patient, tissue was evaluated and micro-dissected by gastrointestinal pathologists (HR and LF), and RNA extraction was performed with miRNeasy FFPE kit (Qiagen) following kit protocol and quantitated by Agilent Bioanalyzer with RNA Nano chip assay in the CUIMC Histopathology Core. Bioanalyzer and nanodrop calculations were performed to determine the quality and quantity of RNA (ng), respectively. RNA was processed using a nanoString assay of 778 genes consisting of the nanoString PanCancer Immune Profiling Panel (730 target genes plus 40 housekeeping genes) and 18 additional genes (Supplemental Table S1). Following hybridization and purification of target-probe complexes, digital counts for each gene-specific target RNA were acquired and normalized to housekeeping genes using nSolver software (nanoString). RNA data were then analyzed using nSolver Advanced Analysis software (nanoString) and R (v 3.3.2).

Spatial analysis

Nearest neighbor and cell counts within radius r were generated by processing inForm (v 2.4.1) output in Python 3.7. Every cell-to-cell Euclidean distance was calculated and stored in a matrix, and phenotypes of interest were selected, resulting in a distance matrix from one cell phenotype population to another. From this matrix, both k nearest neighbor distance and cell counts in a radius of 20 microns were calculated. For k nearest neighbor distance, the mean of the k lowest distances from a cell of phenotype A to every other cell of phenotype B was taken. This was repeated for every cell of phenotype A, and the means were averaged, resulting in the mean distance of the k nearest neighbors from phenotype A to phenotype B. To calculate cell counts in radius, the same distance matrix was used. For a cell of phenotype A, the number of cells of phenotype B which were within a radius of 20 microns was counted, and the frequency of each count (the number of times n cells of phenotype B were observed within 20 microns of phenotype A) was recorded.

Statistical analysis

Patient characteristics were summarized using descriptive statistics: median (range) for continuous variables and frequency (%) for categorical variables. Comparisons between the NT and CRT groups with respect to demographics, clinical characteristics and densities of TILs in tumor, stroma and total image were assessed using chi-squared/Fisher Exact tests and Mann Whitney U tests. Survival comparisons between groups were assessed using Kaplan–Meier curves and Mantel-Cox (Log-rank) tests based on the median for each variable.

Analysis was completed with R (v4.0.2) and GraphPad Prism Version 8.4.0 (GraphPad Software), and statistical significance was defined as $p \leq 0.05$. The RNA was analyzed using differential expression in nSolver advanced analysis software and R (v3.3.2).

Results

Patient characteristics

Patients were selected based on availability of tissue and clinical follow-up. Demographics for both the NT and CRT patients are shown in Table 1. There was a total of 44 resection specimens, including tumors from 26 NT patients and 18 patients treated with CRT prior to surgery. Men and women were distributed similarly between the two groups and median

Table 1. Pancreatic Ductal Adenocarcinoma (PDAC) Patient Characteristics comparing treatment groups. Statistical comparison made using Chi-square/Fisher exact test or t-test analysis (p-values significant at ≤0.05).

Demographics			
Clinical Characteristics	Non-treated (NT)	Neoadjuvant Chemoradiation (CRT)	p-value
Gender	n = 26	n = 18	0.802
Male, no. (%)	14 (53.8)	9 (50.0)	
Female, no. (%)	12 (46.2)	9 (50.0)	
Resectable Diagnosis			
Yes, no. (%)	26 (100)	0 (0)	
No, no. (%)	0 (0)	18 (100)	
Age			0.578
Median, no. (range)	68.5 (51–95)	68 (52–82)	
Pathological Stage*			0.005
IA, no. (%)	0 (0)	2 (11.1)	
IB, no. (%)	1 (3.8)	0 (0)	
IIA, no. (%)	6 (23.1)	12 (66.7)	
IIB, no. (%)	10 (38.5)	3 (16.7)	
III, no. (%)	9 (34.6)	1 (5.5)	
Outcome Characteristics			
Patient Follow-Up (months)			0.428
Median, no. (range)	27 (1–73)	28.5 (8–96)	
OS			
Median Survival (months)	28 (24–49)	37 (17-NA)	
Alive (>2 years), no. (%)	15 (57.7)	10 (55.6)	

*Stages IA and IB were excluded from statistical analysis due to insufficient sample size

ages between groups were comparable (68.5 and 68, respectively), as shown. Patients were diagnosed with PDAC between 2011 and 2016 and feasibility of resection was determined by a multi-disciplinary tumor board. Patients who were deemed resectable had surgery upfront while those initially deemed borderline resectable or locally advanced and were taken to surgery if they had a favorable response to neoadjuvant treatment. Pathologic prognostic stages as per the American Joint Committee on Cancer (AJCC) are shown in Table 1. Pathological stage as per the American Joint Committee on Cancer (AJCC) guidelines was significantly lower in the CRT group at the time of surgery (p = .005), consistent with the fact that these patients successfully responded to neoadjuvant treatment. Median follow-up for the NT group was 27 months (range 1–73 months) with 15 patients alive for longer than 24 months. Median follow-up for the CRT group was 28.5 months (range 8–96 months) with 10 patients alive longer than 24 months. Due to the fact that qmIF, IG (or both) were performed depending on tissue quality and availability, patient demographics separated by analysis cohort (qmIF and IG) are included in Supplemental Table S2. Details regarding chemotherapies received in the CRT patient group are found in Supplemental Table S3.

CRT causes alterations in tumor architecture and increases T cell infiltration

We find that tumors treated with CRT qualitatively have a more dispersed appearance of tumor segments compared to NT patients who have more distinct tumor areas (Figure 1 (a-d)). We evaluated the ratio of total cells in the tumor to total cells in the overall tissue comparing CRT to NT finding less total cells in the tumor areas in specimens from patients treated with CRT (<0.0001; Figure 1(e)). There was a lower total number of dividing cells as assessed by Ki67 positivity in the CRT tumors compared to NT (p = .0067; Figure 1(f)).

We quantified the impact of CRT by comparing immune cell infiltration in the TIME of treated PDACs to NT using qmIF. To quantify T cell infiltration, numbers of cells expressing CD3, a pan T cell marker, were evaluated as a percentage of total nucleated cells across all fields. $CD3^+$ T cells were much more commonly found in both the tumor (p = .0006) and stroma (p = .0078) compartments of CRT treated specimens compared to NT patients (Figure 2(a-b)). The density of $CD3^+$ cells in the total image was also significantly higher (p = .0013) (Figure 2(c)). We further characterized the T cells by analyzing their subgroups, namely cytotoxic T cells (CTLs; $CD3^+CD8^+$), T_h cells ($CD3^+CD4^+FOXP3^-$), and T_{regs} ($CD3^+CD4^+FOXP3^+$) (Figure 2(d-l)). In the tumor compartment of CRT patients (Figure 2(a-j)), significantly elevated densities of $CD3^+$ T cells (p = .0006) (Figure 2(a)), CTLs (p = .0079) (Figure 2(d)), T_h cells (p = .0010) (Figure 2(g)), and Tregs (p = .0089), (Figure 2 (j)) were observed. Although the stromal compartments showed an increase in $CD3^+$ T cells (p = .0078) (Figure 2(b)), T_h cells constituted the only subset that reach statistical significance (p = .022, Figure 2(h)). Surprisingly, density of $CD68^+$ macrophages did not vary with treatment group in either the tumor or stromal compartment (p = .1252 and 0.6171, respectively; Supplemental Figure S2). Median values

for each density analysis are summarized in Supplemental Table S4. Our results demonstrate that CRT resulted in significantly higher densities of infiltrating T cells as compared to NT tumors.

As the tumor compartment was most different comparing CRT and NT tumors, we next focused on the ratio of $CD3^+$ T cells to other cell phenotypes, including macrophages and dividing cells, which were predominately tumor cells based on their location and on their morphology. The ratio of $CD3^+$ T cells/$CD68^+$ cells and the ratio of $CD3^+$ T cells/$Ki67^+$ cells were higher in the tumor compartments of tumors receiving CRT compared to NT tumors (p < .0001, for each ratio; Supplemental Figure S3a-b). We then analyzed the ratio of T_h cells to Tregs, which was also significantly increased in the tumor compartments of CRT tumors relative to NT tumors (p = .026; Supplemental Figure S3c). Comparisons of these ratios in the stromal compartment and total image samples are shown in Supplemental Figure S4.

Increased immune gene expression in tumors treated with CRT compared to NT tumors and normal pancreatic tissue

Next, expression of immunologically relevant genes in PDACs treated with CRT was evaluated in comparison to NT tumors. In a direct comparison of normalized gene expression between treatment groups, 43 of 788 genes examined demonstrate significantly different levels of expression (p < .05, student's T test) (Figure 3(a)). Among these genes, 41 show higher median levels of expression in the CRT group, a result significantly different than is expected from random chance (p < .0001, Fisher's exact test). A heat map with relative levels of expression of these genes is shown (Figure 3(a)).

To further evaluate differential expression between treatment groups, the gene expressions of CRT and NT tumors were compared with that of normal pancreas tissues. Volcano plots demonstrate that there are several genes in the PanCancer Immune Profiling panel that have increased differential expression in cancer specimens regardless of treatment (Supplemental Figure S5). To control for cancer, all duplicated genes that were significantly differentially expressed in both PDAC groups, CRT and NT, when compared to normal (Benjamini Hochberg (BH) 0.05 and $\log_2$ fold change (FC) 0.8 or −0.8) were removed, revealing 49 genes significantly differentially expressed – 19 in NT tumors and 30 in CRT (Figure 3(b-c)). Of the genes with increased expression in CRT treated tumors, all of them were related to either antigen presentation, maturation, migration or modulation of T cells, or induction of inflammatory processes.[35,36] The highest of these were *HLA-DQA1* (FC = 6.6) and *HLA-DQB1* (FC = 5.71). Others include but are not limited to *CCR4, GZMM, CD1A, PRF1, IL2RA, CXCL1, GZMK, IL1R2*, and *CD3D* (Figure 3(b-c)) and Supplemental Table S5.

Impact of T_{reg} cells on survival of CRT patients

We next sought to determine whether the composition of the TIME had an impact on survival. First, no significant difference was found in overall survival between patients receiving NT and CRT (Supplemental Figure S6). In a next step, we closer
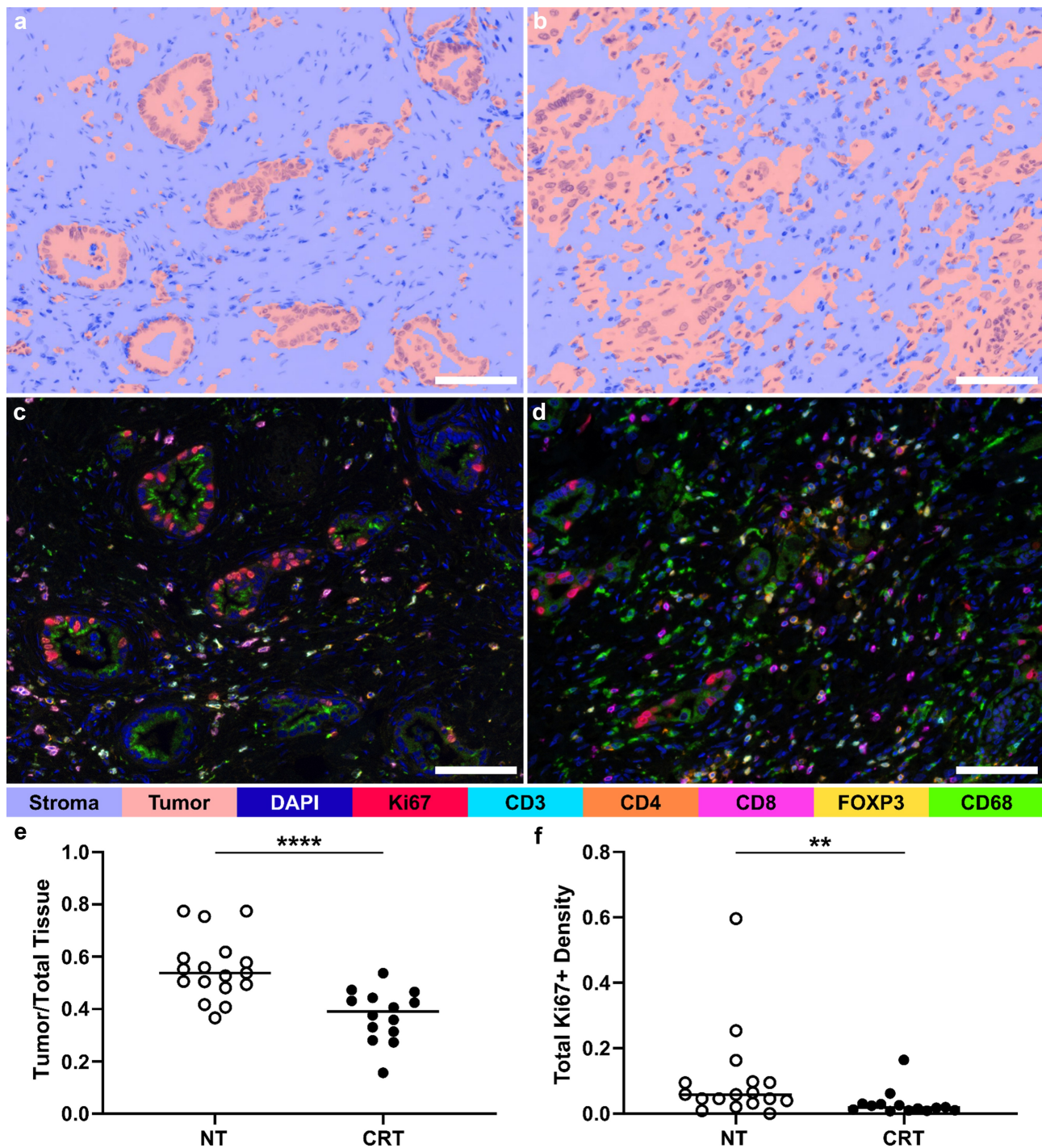
Figure 1. Representative tissue segmentation and multiplex immunofluorescence (mIF) image of a non-treated (NT) patient and a patient who received neoadjuvant chemoradiation (CRT) and analysis of total tumor density. Tissue segmentation images for A) NT and B) CRT. Blue cells are DAPI (nuclei) positive. Red areas represent tumor tissue, blue areas represent stromal tissue. Multiplex view of the same C) NT and D) CRT images stained using mIF for DAPI (nuclei, blue), Ki67 (tumor, proliferative cells, red), CD3 (T cells, cyan), CD4 (T helper cells, (T_h), Orange), CD8 (cytotoxic T cells (CTLs), magenta), FOXP3 (T regulatory cells (Tregs), yellow), CD68 (macrophages, green). White bars represent 100 µm. E) Comparison of the ratio of total cells in the tumor compartment to total cells in the overall tissue sample between treatment groups (p < .0001). F) Comparison of the densities of Ki67$^+$ cells in the total tissue samples between treatment groups (p = .0067). (*≤0.05, **≤0.01, ***≤0.001, ****≤0.0001).

investigated the cohort receiving CRT (n = 14), with eight patients who lived longer than two years and six patients who died within two years. We found that overall T cell densities did not correlate with patient survival (Supplemental Figure S7a). However, patients who died within two years had a significantly higher ratio of T_{regs} per total T cells within the tumor compartment (Figure 4(a)) (p=.0007). CRT treated

patients who had a Treg/CD3 ratio above the median had significantly shorter overall survival (p = .0121; Figure 4(b)). Treg/CD3 ratio was not found to correlate with survival in NT patients (p = .0706; Supplemental Figure 8). Further, survival of CRT treated patients based on median CTL to total T cell ratio was analyzed. We found no significant difference in survival between patients above and below the median CTL
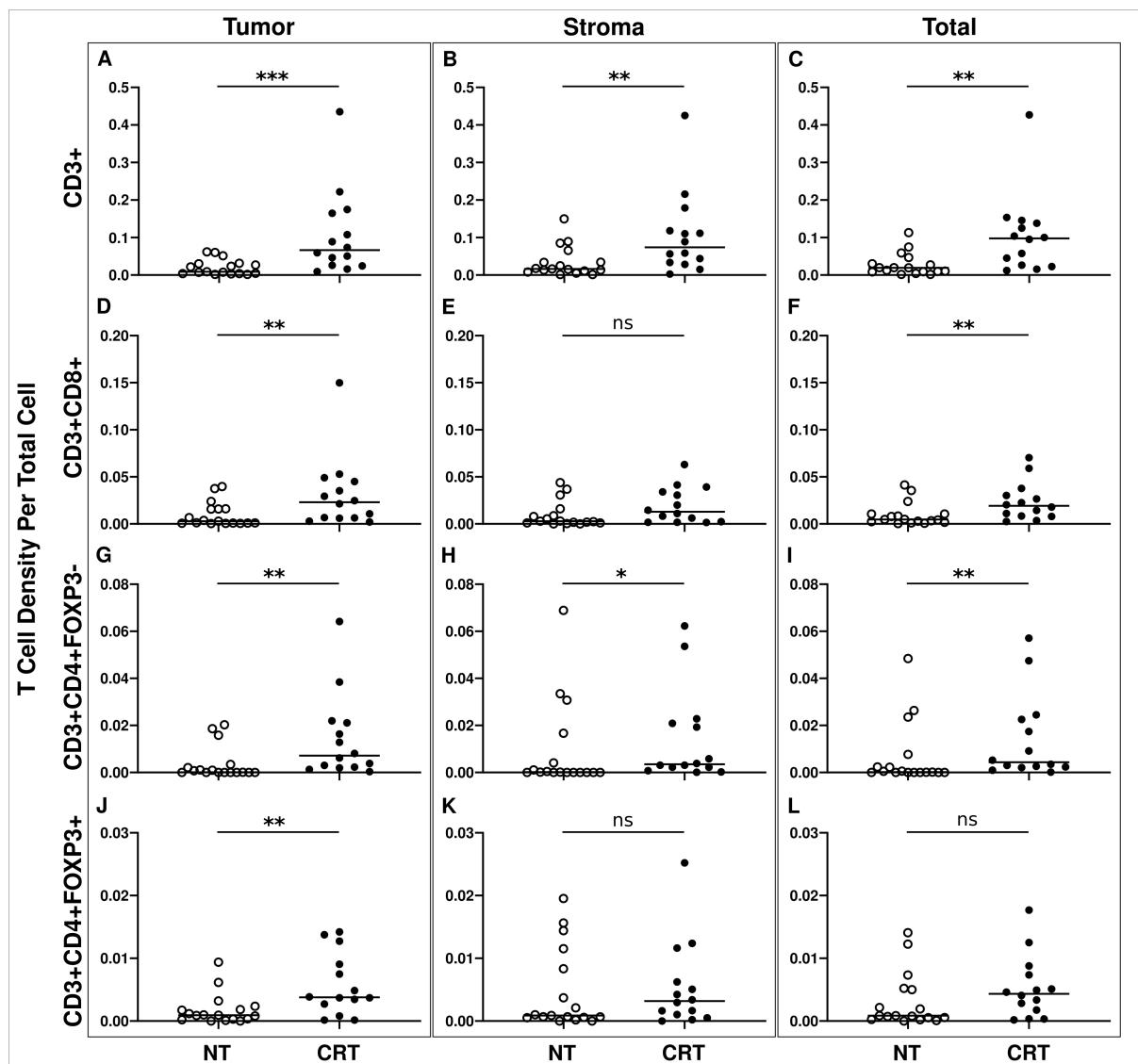
Figure 2. Density of immune cells in tumor, stroma, and total tissue comparing NT to CRT cases. A) CD3$^+$ T cells in tumor (p = .0006), B) CD3$^+$ T cells in stroma (p = .0078), and C) CD3$^+$ T cells in total (p = .0013). D) CD3$^+$CD8$^+$ cytotoxic T cells (CTLs) in tumor (p = .0079), E) CD3$^+$CD8$^+$ CTLs in stroma (p = .0758), and F) CD3$^+$CD8$^+$ CTLs in total (p = .0076). G) CD3$^+$CD4$^+$FOXP3$^-$ T helper (Th) cells in tumor (p = .0010), H) CD3$^+$CD4$^+$FOXP3$^-$ Th cells in stroma (p = .0216), and I) CD3$^+$CD4$^+$FOXP3$^-$ Th cells in total (p = .0078). J) CD3+ CD4+ FOXP3 + T regulatory (Treg) cells in tumor (p = .0089), K) CD3$^+$CD4$^+$FOXP3$^+$ Treg cells in stroma (p = .4211), and L) CD3$^+$CD4$^+$FOXP3$^+$ Treg cells in total (p = .1464). Lines represent median values. (*≤0.05, **≤0.01, ***≤0.001, ****≤0.0001).

to total T cell ratio (Supplemental Figure 7B). Figure 4(c-d) shows representative images exhibiting the difference in the proportion of infiltrating T$_{reg}$ cells to total T cells between a patient who lived >2 years (Figure 4(c)) and a patient who lived <2 years (Figure 4(d)). Our data show that a higher ratio of T$_{regs}$ to CD3 + T cells in the tumor compartment of CRT treated tumors correlate with poor prognosis.

Density and spatial distribution of CD8 + T cells in CRT PDAC compared with treatment naive melanoma

The increase in infiltration by CD8 + T cells induced by CRT was highly significant, and one key question is whether PDAC might hereby be converted into an immunotherapy-responsive "hot tumor."[37] Melanoma is a classic example of a hot tumor, and therefore we sought to investigate how this level of infiltration into irradiated primary PDACs compare with

treatment naive primary melanoma. Clinical data on primary melanoma patients is included in the supplement (Supplemental Table S6). Interestingly, as shown in Figure 5 (a), we find that overall density of CD8 + T cells is similar in melanoma and PDAC, this density only predicts improved prognosis in melanoma and not in PDAC (Supplemental Figure S9). However, the distribution of these cells differs significantly, with CRT PDAC, CD8 + T cells are distributed evenly between tumor and stromal compartments (Figure 5 (b)). Furthermore, the distance between each CD8 + T cell and neighboring CD8 + T cells were significantly closer in melanoma when 1, 5, and 20 nearest neighbors were analyzed (Figure 5(c)) and this difference was significant in the stroma but not in the tumor (Figure 5(d)). In PDAC specimens post CRT, CD8 + T cells are distributed predominantly as single cells throughout tumor and stroma (Figure 5(e)). In contrast to PDAC, melanoma CD8 + T cells are primarily located in the
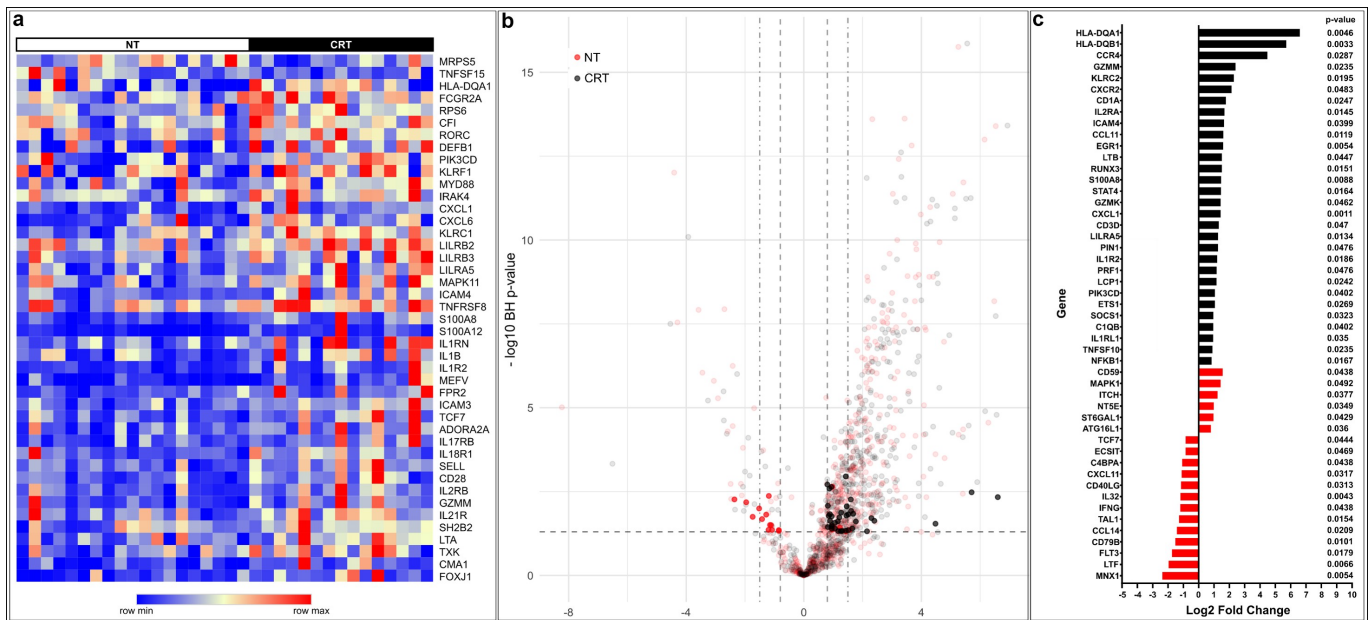
Figure 3. Comparing ratios of T cell subsets within the tumor compartment between NT and CRT. A) CD3^{+} T cell to CD68^{+} macrophage ratio (p < .0001). B) CD3^{+} T cell to Ki67^{+} cell ratio (p < .0001). C) CD3^{+}CD4^{+}FOXP3^{−} T$_h$ cell to CD3^{+}CD4^{+}FOXP3^{+} Treg cell ratio (0.0260). Lines represent median values. (*≤0.05, **≤0.01, ***≤0.001, ****≤0.0001).

stroma, and are clustered together (Figure 5(f)). Further, a higher frequency of CD8 + T cells in CRT PDAC had 0 or only 1 neighboring T cell within 20 microns (Figure 5(g)). These data show that, while overall densities of CD8 + T cells are similar in CRT PDAC compared to primary melanoma, spatial localization of these cells is distinct.

Discussion

Neoadjuvant treatment may increase resectability of PDAC. Beyond that, neoadjuvant treatment may help to control local tumor spread and micrometastasis.[38] Patients with PDAC receiving neoadjuvant treatment have a longer disease-free survival and it was demonstrated that neoadjuvant CRT can prevent local recurrent disease after complete resection.[8,39–42] Immunomodulatory effects of radiation therapy have been postulated in many tumor types. In these tumors, radiation has been shown to cause immunogenic cell death and release of tumor antigens, potentially enhancing anti-tumor immunity.[43–45] In rare cases, when radiation is given to a primary tumor site, distant metastases outside the radiation field also respond to treatment, which is called an abscopal effect and ultimate proof of concept of the induction of anti-tumor immune response by radiation therapy.[46] In a similar fashion, cytotoxic chemotherapies may also increase antigenicity, and, very recently, combining such therapies with immunotherapies have been shown to improve overall survival and progression-free survival in certain cancers – this combinatorial approach was recently FDA approved for this reason.[47–49] PDAC, in contrast, is a uniquely treatment-resistant tumor with only anecdotal evidence of successful generation of anti-tumor immune responses. There is almost no effect of treatment with checkpoint inhibitors such as anti-PD-1/PD-L1 and anti-CTLA-4, either alone or combined in up-front treatment, or together with RT or chemotherapy.[10,50–52]

In our study, tissue samples from patients with borderline resectable or initially locally advanced PDACs, who received CRT followed by surgery were compared with tissue samples from patients with resectable disease who did not receive neoadjuvant treatment. The purpose was to define the impact of CRT on the TIME of PDAC with the use of computational qmIF, qSA, and IG analysis. Our work demonstrates that CRT alters the structure of the TIME, as it induces a substantial influx of T cells, with median T cell count at close to 10% of total cells as compared to approximately 2% total cells in NT patients. There were increases in densities of overall T cells as well as substantial infiltration of CD4^{+} cells, both T$_h$ and Treg cells, and CD8+ CTLs in the TIME. While this suggests that recruitment of T cells is not exclusive to any specific T cell phenotype, this infiltration is primarily concentrated in the tumor compartment. Further, this indicates that CRT increases the potential for direct interaction between tumor cells and T cells, facilitated by the observed alteration to the tumor cellular architecture. Interestingly, no differences in densities of macrophages based on treatment status were observed, suggesting that the high levels of T cells were not reflective of a broader infiltration of myeloid-derived cells. Focusing on the tumor compartment, we evaluated ratios of T cells to other cell phenotypes, including macrophages and dividing cells, as these ratios have been proposed as biomarkers predictive of outcome in other tumor types.[34,53–55] We observed that the overall ratio of T cells to macrophages and dividing cells were significantly increased in the tumor compartments of patients receiving CRT compared to those of NT patients, but we found no evidence that these increased ratios were prognostically significant. While increases in all subsets of T cells were observed, T$_h$ cell to Treg ratio was higher in the tumor compartment of patients receiving CRT. These findings demonstrate alteration in the TIME, which may have relevance for the development of immunotherapeutically active agents.
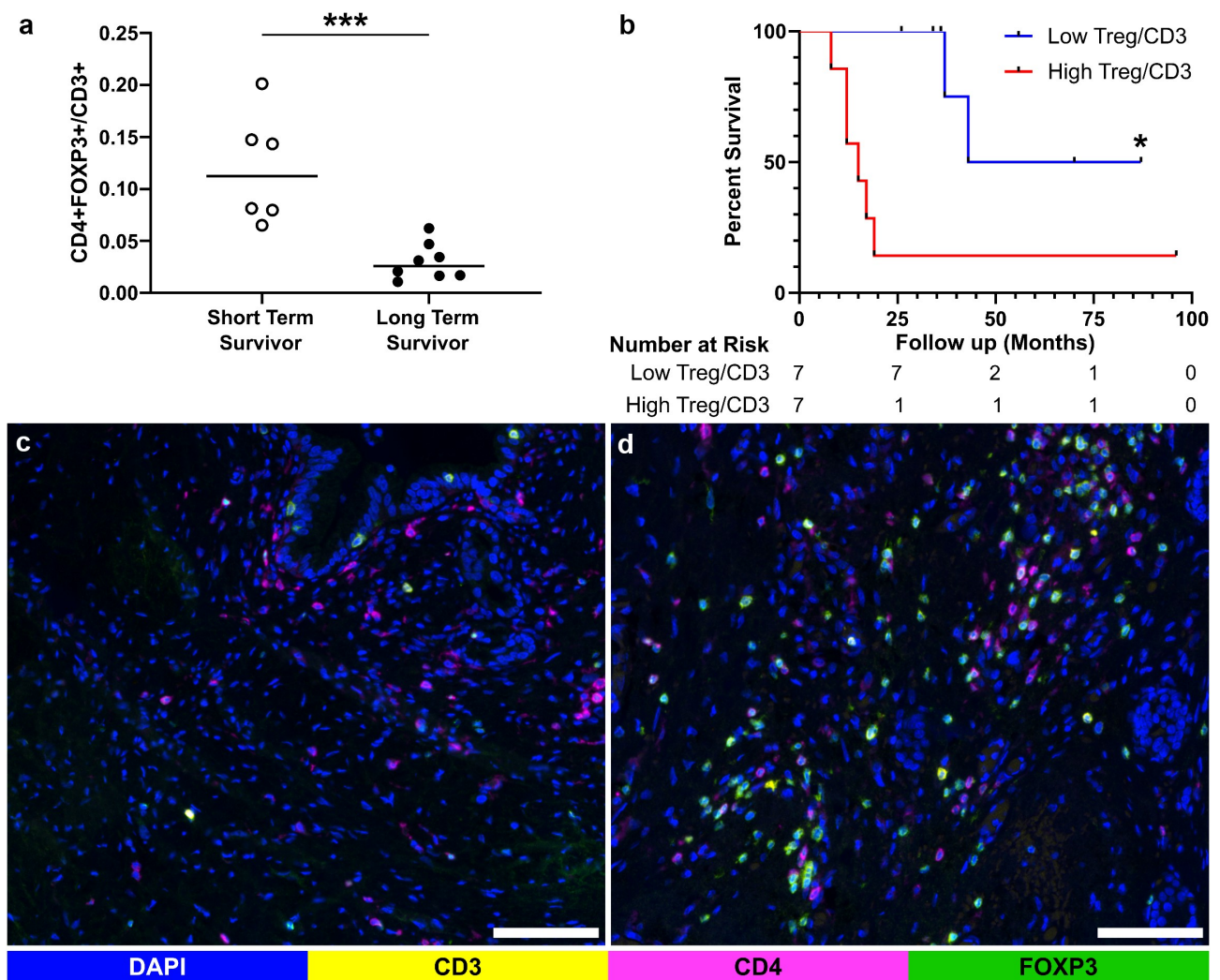
Figure 4. Comparison of overall survival (OS) of CRT treated patients using $CD3^+CD4^+FOXP3^+$ (Treg cell) to $CD3^+$ (T cell) ratio. A) Comparison of the ratios of $CD3^+CD4^+FOXP3^+$ Treg cells to total $CD3^+$ T cells within the tumor compartment between CRT patients who lived <2 years (Short Term Survivor, n = 6) and >2 years (Long Term Survivor, n = 8) after diagnosis (p = .0007). B) Kaplan Meier curve demonstrating the difference in survival between patients with lower (Low Treg/CD3, n = 7) and higher (High Treg/CD3, n = 7) than median $CD3^+CD4^+FOXP3^+$ cell to $CD3^+$ cell ratios (p = .0121 by Mantel-Cox). Representative quantitative mIF images of C) a CRT patient surviving >2 years and D) a CRT patient surviving <2 years stained for DAPI (blue), CD3 (yellow), CD4 (magenta) and FOXP3 (green). White bars represent 100 μm. (*≤0.05, **≤0.01, ***≤0.001, ****≤0.0001).

To evaluate RNA expression of immunologically relevant genes using nanoString in micro-dissected tissues from PDAC patient samples, comparison was done between CRT, NT tumors, and normal pancreatic tissue. T cell genes known to be involved in lymphocyte differentiation, migration, activation, as well as antigen presentation, were found to be overexpressed in the cohort receiving CRT. The genes with the highest relative expression in the CRT group were *HLA-DQA1* (FC = 6.6) and *HLA-DQB1* (FC = 5.7). These genes are part of the Major Histocompatibility Complex II (MHC II) and play a key role in antigen presentation.[36] Other genes found to be strongly induced were *CCR4, GZMM, CD1A, PRF1, IL2RA, CXCL1, GZMK, IL1R2,* and *CD3D*, all of which are associated with T cell trafficking and function. *GZMM* and *PRF1* are known to be expressed by activated CTLs, both of which are directly involved in the destruction of cancer cells.[35] This heightened antigen presentation may correlate with T cell infiltration due to activation of T cells and their proliferation within the TIME.

Despite higher densities of T cell infiltration in the TIME of CRT-treated tumors, patients in the CRT cohort did not live longer than NT patients. As the patient in the CRT cohort were borderline resectable or locally advanced at diagnosis, they were in a higher risk category compared to NT patients. Importantly, only CRT patients who could receive resection were included in this study as tissue was required for analysis. This may suggest a more favorable biology in our CRT cohort compared to borderline resectable cases where resection is not possible post treatment. Our findings are consistent with prior reports of PDAC patients treated with anti-tumor vaccines, in which T cells were coaxed into entering the TIME. The grade of T cell infiltration did not necessarily correlate with prolonged survival in these studies.[56] Similarly, data from this study did not show that T cell infiltration was predictive of survival. Interestingly, however, within the CRT group, patients who had a higher percentage of infiltrating T_{regs} in the tumor compartment had significantly shorter survival relative to patients with T cell infiltrates richer in other T cell subtypes.
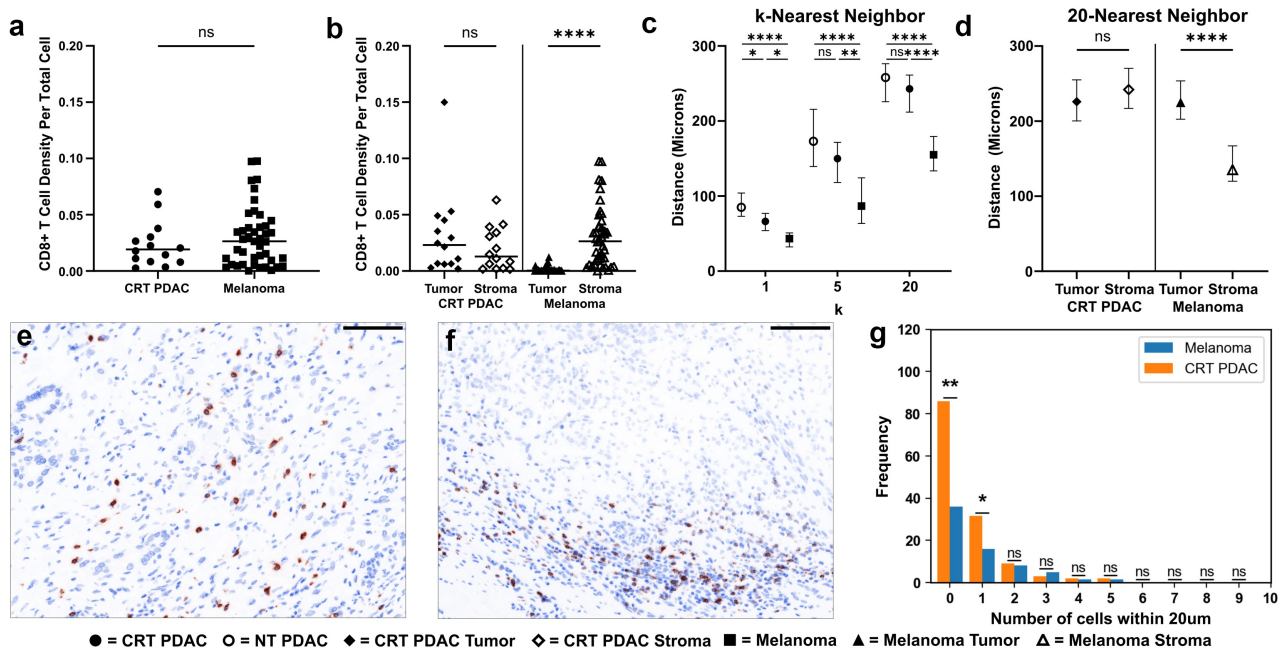
Figure 5. Density, survival, and spatial proximity analysis of CD3+CD8+ cells in CRT PDAC and melanoma. Comparison of CD3+CD8+ cell densities between A) the total tissue compartments of CRT PDAC and melanoma (p = .5267), and B) the tumor and stroma compartments of CRT PDAC (p = .3761) and melanoma (p < .0001), respectively. Lines represent median values. Representative CD8 IHC views of C) CRT PDAC and D) melanoma illustrate the differences in density and spatial profiles of CD8+ cells between the two neoplasms. Black bars represent 100 μm. E) K-nearest neighbor distance analysis was performed for k = 1, k = 5, and k = 20 nearest CD3+CD8+ cells to another CD3+CD8+ cell. The nearest neighbor distances among each neoplasm type were compared for each k using Kruskal-Wallis tests (k = 1, p < .0001; k = 5, p < .0001; k = 20, p < .0001), and the following pairwise distance comparisons were made using Dunn's multiple comparisons test: NT PDAC v. melanoma (k = 1, p < .0001; k = 5, p < .0001; k = 20, p < .0001), NT PDAC v. CRT PDAC (k = 1, p = .0226; k = 5, p = .1593; k = 20, p = .5595), and CRT PDAC v. melanoma (k = 1, p = .0165; k = 5, p = .0011; k = 20, p < .0001). F) Comparison of the average nearest neighbor distances for k = 20 between CD3+CD8+ cells in the stroma and tumor compartments of CRT PDAC (p = .3060) and melanoma (p < .0001), respectively. Data points represent median values, with brackets representing 95% confidence intervals. G) Analysis of the frequency with which a specified number (n) of CD3+CD8+ cells fell within a 20 micron radius of another CD3+CD8+ cell between CRT PDAC and melanoma demonstrated differences for n = 0 (p = .0007) and n = 1 (p = .049). (*≤0.05, **≤0.01, ***≤0.001, ****≤0.0001).

T_{regs} are known to infiltrate pancreatic malignancies very early in oncogenesis and play a key role in establishing an immunosuppressed TIME.[57,58] T_{reg} accumulation also correlates with shortened survival in several PDAC studies, both in tissue[26–29] and in blood.[59–61] Thus, the accumulation of T_{regs} during CRT may be indicative of a more aggressive cancer. Understanding the factors that generate recruitment of T_{regs} versus the recruitment of other T cell subtypes in the TIME of PDAC could markedly improve our ability to develop immunotherapies and combination strategies for this disease.

Given that the objective of many proposed therapies in PDAC is to transform an immunologically "cold" TIME into a "hot" TIME, we compared CRT PDAC to the classic "hot" tumor, melanoma. Melanoma is a highly lethal and aggressive malignancy, but it is highly responsive to immunotherapy. As shown by others, we found that CD8 + T cells in melanoma were primarily located in the tumor stroma,[34] consistent with the hypothesis that, in these progressive tumors requiring surgical resection, CD8 + T cells could not penetrate in high numbers into the tumor tissue itself. Higher numbers of lymphocytes surrounding and penetrating melanomas have been shown to correlate with absence of relapse.[62] In contrast, in PDAC, vaccines are known to increase T cell infiltration but these vaccines do not necessarily prolong survival.[63] Based on our data, the same may be true for CRT. Thus, interestingly, while CRT disrupts tumor architecture and enhances penetration of T cells into the tumor, our data show that these T cells are disparate and do not aggregate with one another, strongly suggesting that additional parameters beyond up-regulation of inflammatory genes and increasing densities of CD8 + T cells characterize a favorable and long-lasting anti-tumor immune response. This is in line with recent data showing that intratumoral lymphoid aggregates correlate with survival in vaccinated patients and further suggests that limited infiltration of T cells into PDAC is only one of multiple barriers to successful anti-tumor immunity.[64] These results should be viewed in the context of the larger literature evaluating the impact of radiation therapy on the TIME, in more immune sensitive tumors such as head and neck cancer where the density of CD8 + T cells was found to correlate with pathologic complete response,[65] in contrast to our data with PDAC. This indicates that treatment impact on the composition of the TIME, as well as TIME-specific predictive immune biomarkers, depend on specific cancer type. Further, reports that radiation increases T cell infiltration and that this infiltration correlates with response to therapy and survival suggest that CD8 + T cell density alone may be a favorable indicator of immune response in more immune sensitive tumors such as melanoma and subsets of breast cancer.[66]

Our work demonstrates that CRT profoundly alters the TIME of PDAC and confirms prior data suggesting that T cell infiltration may not be sufficient to induce anti-tumor immune response in PDACs,[56,67–69] while also suggesting that accumulation of T_{regs} may limit benefit of immune-stimulatory therapies. Limitations of the study include the small sample size and the fact that functional assays could not be performed

on the FFPE samples used. In addition, as this was a retrospective analysis, we were unable to look for systemic immune alterations. Further studies with fresh tissue from surgical resections and patient blood would be useful to characterize the functional status of infiltrating T cell subsets and to isolate and characterize potential anti-tumor antigens. It is well known that heavily mutated and thus immunogenic tumors such as melanoma, non-small cell lung cancers, head and neck cancers, urothelial and bladder cancers respond well to immunotherapies and, even at advanced stages, these therapies can significantly prolong survival.[70–72] Understanding the cellular and molecular mechanisms limiting survival in PDAC patients treated with surgery and maximized perioperative chemotherapy, RT, or CRT will lead to more treatment strategies.

Data Availability Statement

The data that supports the findings of this study are available from the corresponding author upon reasonable request.

Disclosure statement

YMS has recieved funding from Regeneron. BTF has financial interests in both Regeneron and Thermo Fisher Scientific. GAM is a consultant for CEND Biopharma and Synthekine, and has recieved funding from MERCK, Roche, BioLine, and Regeneron. None of the disclosures listed are related to this work.

ORCID

Codruta Chiuzan 🆔 http://orcid.org/0000-0001-8169-5032

References

1. Surveillance. Epidemiology, and end results program (SEER): pancreatic cancer. 2021 ed. Bethesda (MD): National Cancer Institute (NCI). 2021.
2. Rahib L, Smith BD, Aizenberg R, Rosenzweig AB, Fleshman JM, Matrisian LM. Projecting cancer incidence and deaths to 2030: the unexpected burden of thyroid, liver, and pancreas cancers in the United States. Cancer Res. 2014;74(11):2913–2921. doi:10.1158/0008-5472.CAN-14-0155.
3. Janssen QP, O'Reilly EM, van Eijck CHJ, Groot Koerkamp B. Neoadjuvant treatment in patients with resectable and borderline resectable pancreatic cancer. Front Oncol. 2020;10:41. doi:10.3389/fonc.2020.00041.
4. Li D, Xie K, Wolff R, Abbruzzese JL. Pancreatic cancer. Lancet. 2004;363(9414):1049–1057. doi:10.1016/S0140-6736(04)15841-8.
5. Neoptolemos JP, Palmer DH, Ghaneh P, Psarelli EE, Valle JW, Halloran CM, Faluyi O, O'Reilly DA, Cunningham D, Wadsley J, et al. Comparison of adjuvant gemcitabine and capecitabine with gemcitabine monotherapy in patients with resected pancreatic cancer (ESPAC-4): a multicentre, open-label, randomised, phase 3 trial. Lancet. 2017;389(10073):1011–1024. doi:10.1016/S0140-6736(16)32409-6.
6. Conroy T, Hammel P, Hebbar M, Ben Abdelghani M, Wei AC, Raoul J-L, Choné L, Francois E, Artru P, Biagi JJ, et al. FOLFIRINOX or gemcitabine as adjuvant therapy for pancreatic cancer. N Engl J Med. 2018;379(25):2395–2406. doi:10.1056/NEJMoa1809775.
7. Ahmad SA, Duong M, Sohal DPS, Gandhi NS, Beg MS, Wang-Gillam A, Wade JL, Chiorean EG, Guthrie KA, Lowy AM, et al. Surgical outcome results from swog s1505: a randomized clinical trial of mfolfirinox versus gemcitabine/nab-paclitaxel for perioperative treatment of resectable pancreatic ductal adenocarcinoma. Ann Surg. 2020;272(3):481–486. doi:10.1097/SLA.0000000000004155.
8. Tran NH, Sahai V, Griffith KA, Nathan H, Kaza R, Cuneo KC, Shi J, Kim E, Sonnenday CJ, Cho CS, et al. Phase 2 trial of neoadjuvant folfirinox and intensity modulated radiation therapy concurrent with fixed-dose rate-gemcitabine in patients with borderline resectable pancreatic cancer. Int J Radiat Oncol Biol Phys. 2020;106(1):124–133. doi:10.1016/j.ijrobp.2019.08.057.
9. Johnson BA 3rd, Yarchoan M, Lee V, Laheru DA, Jaffee EM. Strategies for increasing pancreatic tumor immunogenicity. Clin Cancer Res. 2017; 23(7):1656–1669. doi:10.1158/1078-0432.CCR-16-2318.
10. O'Reilly EM, Oh DY, Dhani N, Renouf DJ, Lee MA, Sun W, Fisher G, Hezel A, Chang S-C, Vlahovic G, et al. Durvalumab with or without tremelimumab for patients with metastatic pancreatic ductal adenocarcinoma: a phase 2 randomized clinical trial. JAMA Oncol. 2019;5(10):1431. doi:10.1001/jamaoncol.2019.1588.
11. Gibney GT, Kudchadkar RR, DeConti RC, Thebeau MS, Czupryn MP, Tetteh L, Eysmans C, Richards A, Schell MJ, Fisher KJ, et al. Safety, correlative markers, and clinical results of adjuvant nivolumab in combination with vaccine in resected high-risk metastatic melanoma. Clin Cancer Res. 2015;21(4):712–720. doi:10.1158/1078-0432.CCR-14-2468.
12. Hodi FS, O'Day SJ, McDermott DF, Weber RW, Sosman JA, Haanen JB, Gonzalez R, Robert C, Schadendorf D, Hassel JC, et al. Improved survival with ipilimumab in patients with metastatic melanoma. N Engl J Med. 2010;363(8):711–723. doi:10.1056/NEJMoa1003466.
13. Larkin J, Hodi FS, Wolchok JD, Grob JJ, Cowey CL, Lao CD, Schadendorf D, Dummer R, Smylie M, Rutkowski P. Combined nivolumab and ipilimumab or monotherapy in untreated melanoma. N Engl J Med. 2015;373(1):23–34. doi:10.1056/NEJMoa1504030.
14. Weber J, Mandala M, Del Vecchio M, Gogas HJ, Arance AM, Cowey CL, Dalle S, Schenker M, Chiarion-Sileni V, Marquez-Rodas I, et al. Adjuvant nivolumab versus ipilimumab in resected stage III or IV melanoma. N Engl J Med. 2017;377(19):1824–1835. doi:10.1056/NEJMoa1709030.
15. Halbrook CJ, Pasca Di Magliano M, Lyssiotis CA. Tumor crosstalk networks promote growth and support immune evasion in pancreatic cancer. Am J Physiol Gastrointest Liver Physiol. 2018;315(1):G27–G35. doi:10.1152/ajpgi.00416.2017.
16. Ohlund D, Handly-Santana A, Biffi G, Elyada E, Almeida AS, Ponz-Sarvise M, Corbo V, Oni TE, Hearn SA, Lee EJ, et al. Distinct populations of inflammatory fibroblasts and myofibroblasts in pancreatic cancer. J Exp Med. 2017;214(3):579–596. doi:10.1084/jem.20162024.

17. Carstens JL, Correa de Sampaio P, Yang D, Barua S, Wang H, Rao A, Allison JP, LeBleu VS, Kalluri R. Spatial computation of intratumoral T cells correlates with survival of patients with pancreatic cancer. Nat Commun. 2017;8(1):15095. doi:10.1038/ncomms15095.

18. Rodriguez PC, Quiceno DG, Zabaleta J, Ortiz B, Zea AH, Piazuelo MB, Delgado A, Correa P, Brayer J, Sotomayor EM, et al. Arginase I production in the tumor microenvironment by mature myeloid cells inhibits T-cell receptor expression and antigen-specific T-cell responses. Cancer Res. 2004;64 (16):5839–5849. doi:10.1158/0008-5472.CAN-04-0465.

19. Stromnes IM, Hulbert A, Pierce RH, Greenberg PD, Hingorani SR. T-cell localization, activation, and clonal expansion in human pancreatic ductal adenocarcinoma. Cancer Immunol Res. 2017;5 (11):978–991. doi:10.1158/2326-6066.CIR-16-0322.

20. Theate I, van Baren N, Pilotte L, Moulin P, Larrieu P, Renauld J-C, Hervé C, Gutierrez-Roelens I, Marbaix E, Sempoux C, et al. Extensive profiling of the expression of the indoleamine 2,3-dioxygenase 1 protein in normal and tumoral human tissues. Cancer Immunol Res. 2015;3(2):161–172. doi:10.1158/2326-6066.CIR-14-0137.

21. Zhang Y, Yan W, Mathew E, Kane KT, Brannon A 3rd, Adoumie M, Vinta A, Crawford HC, Pasca di Magliano M. Epithelial-Myeloid cell crosstalk regulates acinar cell plasticity and pancreatic remodeling in mice. Elife. 2017;6:e27388. doi:10.7554/eLife.27388.

22. Ye H, Zhou Q, Zheng S, Li G, Lin Q, Wei L, Fu Z, Zhang B, Liu Y, Li Z, et al. Tumor-associated macrophages promote progression and the Warburg effect via CCL18/NF-kB/VCAM-1 pathway in pancreatic ductal adenocarcinoma. Cell Death Dis. 2018;9(5):453. doi:10.1038/s41419-018-0486-0.

23. Wormann SM, Diakopoulos KN, Lesina M, Algül H. The immune network in pancreatic cancer development and progression. Oncogene. 2014;33(23):2956–2967. doi:10.1038/onc.2013.257.

24. Tan HNC, Catedral LIG, San Juan MD. Prognostic significance of tumor-infiltrating lymphocytes on survival outcomes of patients with resected pancreatic ductal adenocarcinoma: a systematic review and meta-analysis. J Immunother. 2020;44:29–40. doi:10.1097/CJI.0000000000000331.

25. Wartenberg M, Cibin S, Zlobec I, Vassella E, Eppenberger-Castori S, Terracciano L, Eichmann MD, Worni M, Gloor B, Perren A, et al. Integrated genomic and immunophenotypic classification of pancreatic cancer reveals three distinct subtypes with prognostic/predictive significance. Clin Cancer Res. 2018;24(18):4444–4454. doi:10.1158/1078-0432.CCR-17-3401.

26. Liu L, Zhao G, Wu W, Rong Y, Jin D, Wang D, Lou W, Qin X. Low intratumoral regulatory T cells and high peritumoral CD8(+) T cells relate to long-term survival in patients with pancreatic ductal adenocarcinoma after pancreatectomy. Cancer Immunol Immunother. 2016;65(1):73–82. doi:10.1007/s00262-015-1775-4.

27. Jiang Y, Du Z, Yang F, Di Y, Li J, Zhou Z, Pillarisetty VG, Fu D. FOXP3+ lymphocyte density in pancreatic cancer correlates with lymph node metastasis. PLoS One. 2014;9(9):e106741. doi:10.1371/journal.pone.0106741.

28. Shibuya KC, Goel VK, Xiong W, Sham JG, Pollack SM, Leahy AM, Whiting SH, Yeh MM, Yee C, Riddell SR, Pillarisetty VG. Pancreatic ductal adenocarcinoma contains an effector and regulatory immune cell infiltrate that is altered by multimodal neoadjuvant treatment. PLoS One. 2014;9(5):e96565. doi:10.1371/journal.pone.0096565.

29. Tang Y, Xu X, Guo S, Zhang C, Tang Y, Tian Y, Ni B, Lu B, Wang H. An increased abundance of tumor-infiltrating regulatory T cells is correlated with the progression and prognosis of pancreatic ductal adenocarcinoma. PLoS One. 2014;9(3):e91551. doi:10.1371/journal.pone.0091551.

30. Vesely MD, Schreiber RD. Cancer immunoediting: antigens, mechanisms, and implications to cancer immunotherapy. Ann N Y Acad Sci. 2013;1284(1):1–5. doi:10.1111/nyas.12105.

31. Fujiwara K, Saung MT, Jing H, Herbst B, Zarecki M, Muth S, Wu A, Bigelow E, Chen L, Li K, et al. Interrogating the immune-modulating roles of radiation therapy for a rational combination with immune-checkpoint inhibitors in treating pancreatic cancer. J Immunother Cancer. 2020;8:e000351.

32. Weisberg SP, Carpenter DJ, Chait M, Dogra P, Gartrell-Corrado RD, Chen AX, Campbell S, Liu W, Saraf P, Snyder ME, et al. Tissue-resident memory t cells mediate immune homeostasis in the human pancreas through the PD-1/PD-L1 pathway. Cell Rep. 2019;29(12):3916–3932 e5. doi:10.1016/j.celrep.2019.11.056.

33. Carpenter DJ, Granot T, Matsuoka N, Senda T, Kumar BV, Thome JJC, Gordon CL, Miron M, Weiner J, Connors T, et al. Human immunology studies using organ donors: impact of clinical variations on immune parameters in tissues and circulation. Am J Transplant. 2018;18(1):74–88. doi:10.1111/ajt.14434.

34. Gartrell RD, Marks DK, Hart TD, Li G, Davari DR, Wu A, Blake Z, Lu Y, Askin KN, Monod A, et al. Quantitative analysis of immune infiltrates in primary melanoma. Cancer Immunol Res. 2018;6(4):481–493. doi:10.1158/2326-6066.CIR-17-0360.

35. Martinez-Lostao L, Anel A, Pardo J. How do cytotoxic lymphocytes kill cancer cells? Clin Cancer Res. 2015;21(22):5047–5056. doi:10.1158/1078-0432.CCR-15-0685.

36. Ting JP, Trowsdale J. Genetic control of MHC class II expression. Cell. 2002Suppl;109(2):S21–33. doi:10.1016/S0092-8674(02)00696-7.

37. Chen DS, Mellman I. Elements of cancer immunity and the cancer-immune set point. Nature. 2017;541(7637):321–330. doi:10.1038/nature21349.

38. Matsuda Y, Ohkubo S, Nakano-Narusawa Y, Fukumura Y, Hirabayashi K, Yamaguchi H, Sahara Y, Kawanishi A, Takahashi S, Arai T, et al. Objective assessment of tumor regression in post-neoadjuvant therapy resections for pancreatic ductal adenocarcinoma: comparison of multiple tumor regression grading systems. Sci Rep. 2020;10(1):18278. doi:10.1038/s41598-020-74067-z.

39. Motoi F, Ishida K, Fujishima F, Ottomo S, Oikawa M, Okada T, Shimamura H, Takemura S, Ono F, Akada M, et al. Neoadjuvant chemotherapy with gemcitabine and S-1 for resectable and borderline pancreatic ductal adenocarcinoma: results from a prospective multi-institutional phase 2 trial. Ann Surg Oncol. 2013;20 (12):3794–3801. doi:10.1245/s10434-013-3129-9.

40. Blair AB, Yin LD, Pu N, Yu J, Groot VP, Rozich NS, Javed AA, Zheng L, Cameron JL, Burkhart RA, Weiss MJ, Wolfgang CL, He J. Recurrence in patients achieving pathological complete response after neoadjuvant treatment for advanced pancreatic cancer. Ann Surg. 2019;274:162–169.

41. Tsuchiya N, Matsuyama R, Murakami T, Yabushita Y, Sawada YU, Kumamoto T, ENDO I. Risk factors associated with early recurrence of borderline resectable pancreatic ductal adenocarcinoma after neoadjuvant chemoradiation therapy and curative resection. Anticancer Res. 2019;39(8):4431–4440. doi:10.21873/anticanres.13615.

42. Wittmann D, Hall WA, Christians KK, Barnes CA, Jariwalla NR, Aldakkak M, Clarke CN, George B, Ritch PS, Riese M, et al. Impact of neoadjuvant chemoradiation on pathologic response in patients with localized pancreatic cancer. Front Oncol. 2020;10:460. doi:10.3389/fonc.2020.00460.

43. Vanpouille-Box C, Alard A, Aryankalayil MJ, Sarfraz Y, Diamond JM, Schneider RJ, Inghirami G, Coleman CN, Formenti SC, Demaria S, et al. DNA exonuclease trex1 regulates radiotherapy-induced tumour immunogenicity. Nat Commun. 2017;8(1):15618. doi:10.1038/ncomms15618.

44. Galluzzi L, Buque A, Kepp O, Zitvogel L, Kroemer G. Immunological effects of conventional chemotherapy and targeted anticancer agents. Cancer Cell. 2015;28(6):690–714. doi:10.1016/j.ccell.2015.10.012.

45. Mathew M, Enzler T, Shu CA, Rizvi NA. Combining chemotherapy with PD-1 blockade in NSCLC. Pharmacol Ther. 2018;186:130–137. doi:10.1016/j.pharmthera.2018.01.003.

46. Ngwa W, Irabor OC, Schoenfeld JD, Hesser J, Demaria S, Formenti SC. Using immunotherapy to boost the abscopal effect. Nat Rev Cancer. 2018;18(5):313–322. doi:10.1038/nrc.2018.6.

47. Gandhi L, Rodriguez-Abreu D, Gadgeel S, Esteban E, Felip E, De Angelis F, Domine M, Clingan P, Hochmair MJ, Powell SF, et al. Pembrolizumab plus chemotherapy in metastatic non-small-cell lung cancer. N Engl J Med. 2018;378(22):2078–2092. doi:10.1056/NEJMoa1801005.

48. Burtness B, Harrington KJ, Greil R, Soulières D, Tahara M, de Castro G, Psyrri A, Basté N, Neupane P, Bratland Å, et al. Pembrolizumab alone or with chemotherapy versus cetuximab with chemotherapy for recurrent or metastatic squamous cell carcinoma of the head and neck (KEYNOTE-048): a randomised, open-label, phase 3 study. Lancet. 2019;394(10212):1915–1928. doi:10.1016/S0140-6736(19)32591-7.

49. Fang W, Yang Y, Ma Y, Hong S, Lin L, He X, Xiong J, Li P, Zhao H, Huang Y, et al. Camrelizumab (SHR-1210) alone or in combination with gemcitabine plus cisplatin for nasopharyngeal carcinoma: results from two single-arm, phase 1 trials. Lancet Oncol. 2018;19 (10):1338–1350. doi:10.1016/S1470-2045(18)30495-9.

50. Weiss GJ, Blaydorn L, Beck J, Bornemann-Kolatzki K, Urnovitz H, Schütz E, Khemka V. Phase Ib/II study of gemcitabine, nab-paclitaxel, and pembrolizumab in metastatic pancreatic adenocarcinoma. Invest New Drugs. 2018;36(1):96–102. doi:10.1007/s10637-017-0525-1.

51. Macherla S, Laks S, Naqash AR, Bulumulle A, Zervos E, Muzaffar M. Emerging role of immune checkpoint blockade in pancreatic cancer. Int J Mol Sci. 2018;19(11):3505. doi:10.3390/ijms19113505.

52. Brahmer JR, Tykodi SS, Chow LQ, Hwu W-J, Topalian SL, Hwu P, Drake CG, Camacho LH, Kauh J, Odunsi K, et al. Safety and activity of anti-PD-L1 antibody in patients with advanced cancer. N Engl J Med. 2012;366(26):2455–2465. doi:10.1056/NEJMoa1200694.

53. Acs B, Ahmed FS, Gupta S, Wong PF, Gartrell RD, Sarin Pradhan J, Rizk EM, Gould Rothberg B, Saenger YM, Rimm DL, et al. An open source automated tumor infiltrating lymphocyte algorithm for prognosis in melanoma. Nat Commun. 2019;10(1):5440. doi:10.1038/s41467-019-13043-2.

54. Peranzoni E, Lemoine J, Vimeux L, Feuillet V, Barrin S, Kantari-Mimoun C, Bercovici N, Guérin M, Biton J, Ouakrim H, et al. Macrophages impede CD8 T cells from reaching tumor cells and limit the efficacy of anti-PD-1 treatment. Proc Natl Acad Sci U S A. 2018;115(17):E4041–E4050. doi:10.1073/pnas.1720948115.

55. Mahajan UM, Langhoff E, Goni E, Costello E, Greenhalf W, Halloran C, Ormanns S, Kruger S, Boeck S, Ribback S, et al. Immune cell and stromal signature associated with progression-free survival of patients with resected pancreatic ductal adenocarcinoma. Gastroenterology. 2018;155(5):1625–1639 e2. doi:10.1053/j.gastro.2018.08.009.

56. Lutz ER, Wu AA, Bigelow E, Sharma R, Mo G, Soares K, Solt S, Dorman A, Wamwea A, Yager A, et al. Immunotherapy converts nonimmunogenic pancreatic tumors into immunogenic foci of immune regulation. Cancer Immunol Res. 2014;2(7):616–631. doi:10.1158/2326-6066.CIR-14-0027.

57. Keenan BP, Saenger Y, Kafrouni MI, Leubner A, Lauer P, Maitra A, Rucki AA, Gunderson AJ, Coussens LM, Brockstedt DG, et al. A listeria vaccine and depletion of T-regulatory cells activate immunity against early stage pancreatic intraepithelial neoplasms and prolong survival of mice. Gastroenterology. 2014;146(7):1784–94 e6. doi:10.1053/j.gastro.2014.02.055.

58. Roth S, Zamzow K, Gaida MM, Heikenwälder M, Tjaden C, Hinz U, Bose P, Michalski CW, Hackert T. Evolution of the immune landscape during progression of pancreatic intraductal papillary mucinous neoplasms to invasive cancer. EBioMedicine. 2020;54:102714. doi:10.1016/j.ebiom.2020.102714.

59. Ikemoto T, Shimada M, Ishikawa D, Kawashita Y, Teraoku H, Yoshikawa M, Yamada S, Saito YU, Morine Y, Imura S, et al. Peripheral tr1 and foxp3(+) treg as markers of recurrent malignancies in patients with hepato-biliary pancreatic cancers. Anticancer Res. 2017;37(10):5541–5552. doi:10.21873/anticanres.11986.

60. Liu C, Cheng H, Luo G, Lu Y, Jin K, Guo M, Ni Q, Yu X. Circulating regulatory T cell subsets predict overall survival of patients with unresectable pancreatic cancer. Int J Oncol. 2017;51 (2):686–694. doi:10.3892/ijo.2017.4032.

61. Cheng H, Luo G, Lu Y, Jin K, Guo M, Xu J, Long J, Liu L, Yu X, Liu C, et al. The combination of systemic inflammation-based marker NLR and circulating regulatory T cells predicts the prognosis of resectable pancreatic cancer patients. Pancreatology. 2016;16(6):1080–1084. doi:10.1016/j.pan.2016.09.007.

62. Azimi F, Scolyer RA, Rumcheva P, Moncrieff M, Murali R, McCarthy SW, Saw RP, Thompson JF. Tumor-infiltrating lymphocyte grade is an independent predictor of sentinel lymph node status and survival in patients with cutaneous melanoma. J Clin Oncol. 2012;30 (21):2678–2683. doi:10.1200/JCO.2011.37.8539.

63. Le DT, Picozzi VJ, Ko AH, Wainberg ZA, Kindler H, Wang-Gillam A, Oberstein P, Morse MA, Zeh HJ, Weekes C, et al. Results from a phase iib, randomized, multicenter study of GVAX pancreas and CRS-207 compared with chemotherapy in adults with previously treated metastatic pancreatic adenocarcinoma (ECLIPSE study). Clin Cancer Res. 2019;25(18):5493–5502. doi:10.1158/1078-0432.CCR-18-2992.

64. Zheng L, Ding D, Edil BH, Judkins C, Durham JN, Thomas DL 2nd, Bever KM, Mo G, Solt SE, Hoare JA, et al. Vaccine-induced intratumoral lymphoid aggregates correlate with survival following treatment with a neoadjuvant and adjuvant vaccine in patients with resectable pancreatic adenocarcinoma. Clin Cancer Res. 2021;27 (5):1278–1286. doi:10.1158/1078-0432.CCR-20-2974.

65. Hecht M, Gostian AO, Eckstein M, Rutzner S, von der Grün J, Illmer T, Hautmann MG, Klautke G, Laban S, Brunner T, et al. Safety and efficacy of single cycle induction treatment with cisplatin/docetaxel/durvalumab/tremelimumab in locally advanced HNSCC: first results of checkRad-CD8. J Immunother Cancer. 2020;8(2):e001378. doi:10.1136/jitc-2020-001378.

66. Formenti SC, Demaria S. Systemic effects of local radiotherapy. Lancet Oncol. 2009;10(7):718–726. doi:10.1016/S1470-2045(09)70082-8.

67. Liu S, Zhang W, Liu K, Wang Y. CD160 expression on CD8(+) T cells is associated with active effector responses but limited activation potential in pancreatic cancer. Cancer Immunol Immunother. 2020;69(5):789–797. doi:10.1007/s00262-020-02500-3.

68. Peng J, Sun BF, Chen CY, Zhou J-Y, Chen Y-S, Chen H, Liu L, Huang D, Jiang J, Cui G-S, et al. Author correction: single-cell RNA-seq highlights intra-tumoral heterogeneity and malignant progression in pancreatic ductal adenocarcinoma. Cell Res. 2019;29(9):777. doi:10.1038/s41422-019-0212-1.

69. Peng J, Sun BF, Chen CY, Zhou JY, Chen YS, Chen H, Liu L, Huang D, Jiang J, Cui GS, et al. Single-cell RNA-seq highlights intra-tumoral heterogeneity and malignant progression in pancreatic ductal adenocarcinoma. Cell Res. 2019;29(9):725–738. doi:10.1038/s41422-019-0195-y.

70. Wolchok JD, Chiarion-Sileni V, Gonzalez R, Rutkowski P, Grob J-J, Cowey CL, Lao CD, Wagstaff J, Schadendorf D, Ferrucci PF, et al. Overall survival with combined nivolumab and ipilimumab in advanced melanoma. N Engl J Med. 2017;377 (14):1345–1356. doi:10.1056/NEJMoa1709684.

71. Alexandrov LB, Nik-Zainal S, Wedge DC, Aparicio SAJR, Behjati S, Biankin AV, Bignell GR, Bolli N, Borg A, Børresen-Dale A-L, et al. Signatures of mutational processes in human cancer. Nature. 2013;500(7463):415–421. doi:10.1038/nature12477.

72. Samstein RM, Lee CH, Shoushtari AN, Hellmann MD, Shen R, Janjigian YY, Barron DA, Zehir A, Jordan EJ, Omuro A, et al. Tumor mutational load predicts survival after immunotherapy across multiple cancer types. Nat Genet. 2019;51(2):202–206. doi:10.1038/s41588-018-0312-8.